J Nanostruct 16(3): 3257-3269, Summer 2026

RESEARCH PAPER

Foliar Nano-Fertilization with ZnO and Fe_2O_3 Nanoparticles Enhances Phytochemical Quality and Antioxidant Capacity of Ocimum basilicum L.

Ansam Fouad Ahmed [1], Marawh Hakim Turkl [2] and Alhan Hamid Faisal [3]*

[1] *Forensic Science Department, College of Science, University of Al-Qadisiyah, Diwaniyah, Iraq*

[2] *Department of Environment, College of Science, University of AL-Qadisiyah, Iraq*

[2] *Department of Basic Science, College of Dentistry, University of AL-Qadisiyah, Iraq*

ARTICLE INFO

Article History:
Received 20 March 2026
Accepted 17 May 2026
Published 01 July 2026

Keywords:
Antioxidant enzymes
Essential oil
Foliar application
Iron oxide nanoparticles
Medicinal plants
Zinc oxide nanoparticles

ABSTRACT

The study examined the impact of ZnO and Fe_2O_3-nanoparticles on growth, metabolite buildup, and antioxidant enzyme activity in three sweet basil cultivars (Ocimum basilicum L.). A factorial randomised complete block arrangement was duplicated three times in the 2025 season study. ZnO-NPs and Fe_2O_3-NPs were foliar sprayed on Dark Opal, Genovese, and Cinnamon basil cultivars at 0, 50, 100, and 150mg.L^{-1}; nanomaterials were characterised using SEM and XRD. Increased plant height, leaf number, shoot biomass, and chlorophyll levels were observed with both nanoparticle types, with the most consistent morphological benefits across cultivars at 100mg.L^{-1} ZnO-NPs. After treatment, carbohydrates, proteins, and free amino acids increased significantly. Fe_2O_3-NPs at 100mg.L^{-1} significantly increased secondary metabolism, including phenolics, flavonoids, and essential oils. CAT, POD, and SOD activities increased in treated plants, and GC-MS profiling showed bioactive chemical variations between treatments and cultivars. While cultivar x treatment interaction was significant for most variables, Dark Opal was the most responding cultivar. The study suggests that foliar sprays of ZnO-NPs and Fe_2O_3-NPs can improve the growth and phytochemical value of sweet basil, potentially for medicinal plant production.

How to cite this article
Fouad Ahmed A., Hakim Turkl M., Hamid Faisal A. Foliar Nano-Fertilization with ZnO and Fe_2O_3 Nanoparticles Enhances Phytochemical Quality and Antioxidant Capacity of Ocimum basilicum L.. J Nanostruct, 2026; 16(3):3257-3269. DOI: 10.22052/JNS.2026.03.021

INTRODUCTION

Sweet basil (Ocimum basilicum L.) is a member of the family Laminaceae and is cultivated in tropical and subtropical countries for its aromatic and medicinal characteristics. These are antioxidant, antibacterial, anti-inflammatory and anticancer. Its bioactive ingredients are alkaloids, phenolics, flavonoids, tannins, saponins and essential oils. Basil essential oil has more than 200 chemical components, mainly linalool, eugenol, estragole and eucalyptol. The oil is appreciated in clinical, cosmetic and food industries [1, 2]. Bioactive substances of plant origin are being investigated for the treatment of several clinical problems such as metabolic abnormalities, including paediatric obesity [3], gastrointestinal

* *Corresponding Author Email: ansam.fouad@qu.edu.iq*

disorders in paediatric patients [4], and oxidative stress-related diseases [5]. Nanotechnology has also been used to increase agricultural production and modification of secondary metabolism. Nanoparticles are of size (1-100 nm), high surface-to-volume ratio and high reactivity, which allows them to tightly interact with the plant cellular machinery [6, 7]. Recent studies have shown that metal-oxide nanoparticles can activate defense-related signalling pathways and increase the production of secondary metabolites in medicinal species [8, 9]. Zinc is a micronutrient involved in photosynthesis, chlorophyll production, and activation of enzymes. Application of Zinc to the leaves has been demonstrated to boost growth and levels of bioactive compounds in medicinal plants [10, 11]. Iron oxide nanoparticles (Fe-O-NPs) help in improving plant performance through food delivery and stress signalling by increasing chlorophyll production, antioxidant enzymes and secondary metabolite biosynthesis [12, 13]. Iron is an essential element for human health, and disorders of iron homeostasis are associated with clinical diseases such as β-thalassemia and its ophthalmic sequelae [14, 15]. Nanoparticles induce reactive oxygen species (ROS) that activate enzymatic and non-enzymatic antioxidant networks and stimulate the formation of phenolics, flavonoids and terpenoids. The effects of nanoparticles depend on the type of particle, its concentration, the plant species and the cultivar, thus each application needs to be studied to achieve optimisation. Although there are a lot of data about the impacts of nanoparticles on agricultural crops, we know very little about the effects of ZnO-NPs and Fe2O3-NPs on different basil cultivars. The present study was therefore designed to assess foliar applications of these two nanoparticles, at different concentrations, on growth, primary and secondary metabolites, antioxidant enzyme activities, and phytochemical profiles of three O. basilicum cultivars, with the broader aim of refining nano-fertilization strategies in medicinal plant production.

MATERIALS AND METHODS

Experimental Site and Design

The experiment was carried out during the 2025 growing season in the research greenhouse of the College of Agriculture. A factorial randomized complete block design (RCBD) was used, with three replications. The first factor consisted of three sweet basil (Ocimum basilicum L.) cultivars, namely Dark Opal (purple-leafed), Genovese (green-leafed), and Cinnamon basil. The second factor was the foliar treatment with ZnO-NPs and Fe_2O_3-NPs, applied at concentrations of 0, 50, 100, and 150 mg L^{-1}. Plants in the control group were sprayed with distilled water only.

Plant Material and Growing Conditions

Seeds of the three basil cultivars were first surface-sterilized with 1% sodium hypochlorite for 5 min, then rinsed several times with sterile distilled water and sown in plastic trays filled with a peat moss/perlite mixture (2:1, v/v). After about four weeks, uniform seedlings bearing 4–6 true leaves were transplanted into 25 cm diameter plastic pots containing sandy loam soil amended with organic matter (3:1). Throughout the experiment, plants were grown under natural photoperiod, with day/night temperatures of 25 ± 2 °C / 18 ± 2 °C and relative humidity in the range of 60–70%. Selected physicochemical properties of the experimental soil are summarized in Table 1.

Nanoparticle Characterization

Iron oxide nanoparticles (Fe2O3-NPs, >98% purity) and zinc oxide nanoparticles (ZnO-NPs, >99% purity) were acquired from Sigma-Aldrich (USA). Particle morphology was examined with a scanning electron microscope (TESCAN MIRA3, 15kV). XRD (Bruker D8 Advance) using Cu-Kα. radiation (XRD) was used to determine the crystalline structure and the Debye–Scherrer equation was used to calculate the crystallite size.

Nanoparticle Application

To ensure nanoparticle dispersion, stock suspensions were made by dispersing in deionised water and sonicating for 30 min. Before each spray, 50, 100, and 150 mg L^{-1} working concentrations were diluted with 0.1% Tween-20 as a surfactant. At 30, 45, and 60 days after transplanting (DAT), a hand-held sprayer was used to fully wet the leaves with 50 mL of solution per plant.

Growth Parameters

Five plants from each treatment were randomly selected and measured at 75 DAT. Plant height was measured from soil surface to tip of main stem and number of leaves was counted manually. Fresh weights of shoot and root were acquired

immediately after harvesting and dry weights were obtained after drying the samples in an oven for 48 h at 70 °C until constant weight was reached.

Photosynthetic Pigments

Following Lichtenthaler and Wellburn [16], fresh leaf tissue (0.5 g) was extracted in 80% acetone for chlorophyll and carotenoid pigments. After reading absorbance at 663, 645, and 470 nm using a UV-Vis spectrophotometer, pigment content was determined using established equations and represented in mg g^{-1} fresh weight.

Primary Metabolites Analysis

The anthrone approach [17] assessed total carbohydrate content using glucose as the reference and 620 nm absorption. BSA was used as a standard at 595 nm in the Bradford assay [18] to quantify total protein. Ninhydrin was used to measure free amino acids [19], with glycine as the calibration standard at 570 nm.

Secondary Metabolites Analysis

Total phenolic content (TPC) was assayed by the Folin–Ciocalteu method [20] and expressed as mg gallic acid equivalents (GAE) g^{-1} dry weight. Total flavonoid content (TFC) was determined using the aluminium chloride colorimetric assay [21] and reported as mg quercetin equivalents (QE) g^{-1} dry weight. Essential oil was extracted by hydrodistillation in a Clevenger-type apparatus for 3 h.

Antioxidant Enzyme Activities

Fresh leaf material (0.5 g) was homogenized in 50 mM phosphate buffer (pH 7.0) supplemented with 1 mM EDTA and 1% PVP at 4 °C, and the homogenate was centrifuged at 12,000 rpm for 20 min. Catalase (CAT) activity was determined by following the decomposition of H_2O_2 at 240 nm [22]. Peroxidase (POD) activity was measured by the guaiacol oxidation method, with absorbance read at 470 nm [23], whereas superoxide dismutase (SOD) activity was assessed on the basis of inhibition of NBT photochemical reduction at 560 nm [24].

GC-MS Analysis

Methanolic extracts were obtained by macerating dried leaf powder (5 g) in 50 mL of methanol for 72 h. GC-MS analysis was then performed on an Agilent 7890B gas chromatograph coupled with an Agilent 5977A mass detector, fitted with an HP-5MS capillary column (30 m × 0.25 mm × 0.25 µm). The oven program started at 50 °C (held for 2 min), then was ramped at

Table 1. Physicochemical properties of experimental soil.

Parameter	Value
Soil texture	Sandy loam
pH	7.2
EC (dS m^{-1})	1.8
Organic matter (%)	1.5
Available N (mg kg^{-1})	45.2
Available P (mg kg^{-1})	12.8
Available K (mg kg^{-1})	185.4

Table 2. Crystallographic parameters of ZnO-NPs and Fe_2O_3-NPs determined by XRD analysis.

Nanoparticle	2θ (degree)	Crystal Plane (hkl)	d-spacing (Å)	Crystallite Size (nm)	Crystal Structure
ZnO-NPs	31.77	(100)	2.814	32.5 ± 2.3	Hexagonal wurtzite
	34.42	(002)	2.603		
	36.25	(101)	2.476		
Fe_2O_3-NPs	24.14	(012)	3.684	41.8 ± 3.1	Rhombohedral hematite
	33.15	(104)	2.700		
	35.61	(110)	2.519		

5 °C min^{-1} up to 280 °C and held for 10 min. Identification of compounds was carried out using the NIST library database.

Statistical Analysis

Statistical analysis of the data was carried out using ANOVA in SAS software (version 9.4), and treatment means were compared by Duncan's Multiple Range Test at $p \leq 0.05$. All results are reported as mean ± standard error of three replications.

RESULTS AND DISCUSSION

Nanoparticle Characterization

Scanning electron microscopy (SEM) revealed clear morphological differences between the two types of nanoparticles. The ZnO-NPs were mostly spherical to hexagonal in shape, with particle sizes ranging from about 25 to 45 nm, whereas the Fe_2O_3-NPs displayed a more irregular spherical morphology, with sizes between 30 and 55 nm (Fig. 1). These features are in good agreement with earlier observations made by Yousaf et al. [13], who reported similar morphological characteristics for iron oxide nanoparticles. The fact that both nanoparticle types showed a relatively uniform size distribution suggests that the synthesis quality was adequate for agricultural use.

XRD patterns showed the crystalline structure of both nanoparticle forms (Fig. 2). The ZnO-NPs

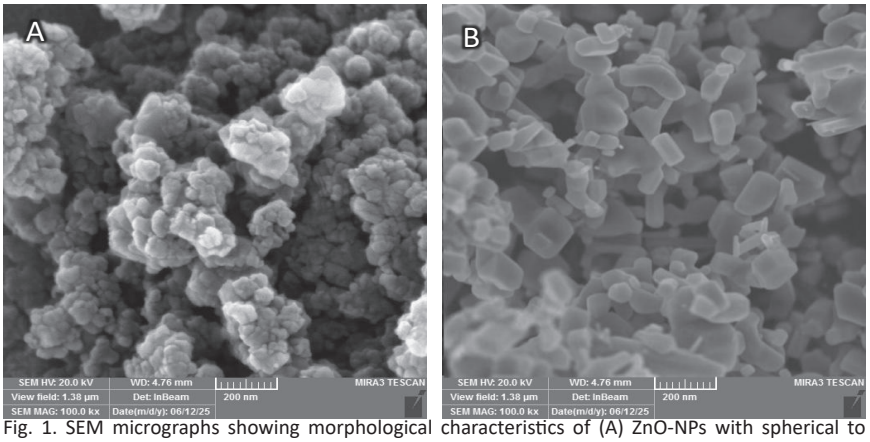

Fig. 1. SEM micrographs showing morphological characteristics of (A) ZnO-NPs with spherical to hexagonal shape and (B) Fe_2O_3-NPs with irregular spherical morphology. Scale bar = 100 nm.

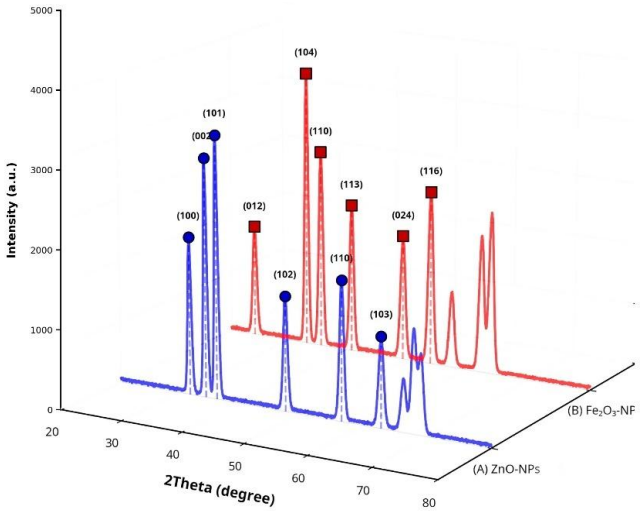

Fig. 2. XRD diffraction patterns of (A) ZnO-NPs showing hexagonal wurtzite structure and (B) Fe_2O_3-NPs showing rhombohedral hematite phase.

showed diffraction peaks at 31.77°, 34.42°, 36.25°, 47.54°, and 56.60°, matching to the hexagonal wurtzite structure (JCPDS card no. 36-1451). For the Fe_2O_3-NPs, peaks were observed at 24.14°, 33.15°, 35.61°, 40.85°, and 49.48°, which can be assigned to the (012), (104), (110), (113), and (024) planes of the rhombohedral hematite phase (JCPDS card no. 33-0664). Average crystallite sizes, estimated from the Debye–Scherrer equation, were 32.5 nm for ZnO-NPs and 41.8 nm for Fe_2O_3-NPs (Table 2).

Effect of Nanoparticles on Vegetative Growth Parameters

Plant Height and Leaf Number

The statistical analysis indicated significant effects ($p \leq 0.05$) of nanoparticle treatments, cultivar, and their interaction on plant height as well as leaf number (Table 3). Foliar applications of both ZnO-NPs and Fe_2O_3-NPs led to clear increases in plant height when compared with untreated controls. The tallest plants (58.7 cm) were observed in the Dark Opal cultivar treated with 100 mg L^{-1} ZnO-NPs, which corresponded to a 47.3% increase relative to the control (39.8 cm). Genovese, on the other hand, responded most strongly to Fe_2O_3-NPs at 100 mg L^{-1}, reaching a height of 52.4 cm against 37.2 cm in the control.

The improvement in plant height observed after nanoparticle treatment can largely be explained by enhanced nutrient uptake and improved photosynthetic efficiency. Zinc, in particular, acts as an essential cofactor for several enzymes involved in auxin metabolism, most notably tryptophan synthase, which catalyzes the formation of indole-3-acetic acid (IAA) [11] (Fig. 3). The cultivar-dependent pattern of response further suggests that there is genetic variability among cultivars in terms of nanoparticle uptake and the efficiency with which these nanomaterials

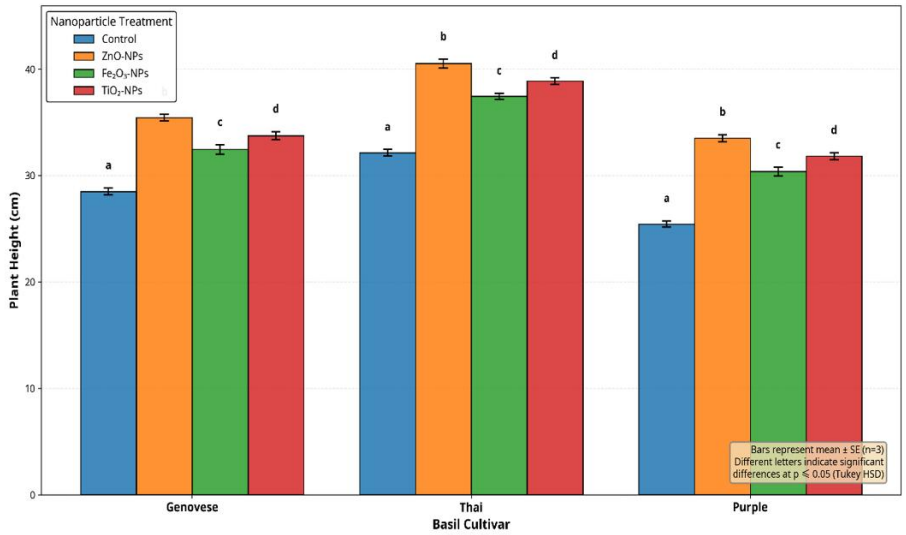

Fig. 3. Comparative effect of nanoparticle treatments on plant height among three basil cultivars. Bars represent mean ± SE (n=3). Different letters indicate significant differences at $p \leq 0.05$.

Table 3. Effect of ZnO-NPs and Fe_2O_3-NPs foliar application on plant height (cm) and number of leaves of three Ocimum basilicum L. cultivars.

Treatment (mg L^{-1})	Dark Opal Height	Dark Opal Leaves	Genovese Height	Genovese Leaves	Cinnamon Height	Cinnamon Leaves
Control	39.8 ± 1.2 f	98.7 ± 4.2 g	37.2 ± 1.4 f	87.3 ± 3.8 h	35.6 ± 1.1 f	82.5 ± 3.5 h
ZnO-NPs 50	48.3 ± 1.5 d	125.4 ± 5.1 e	44.6 ± 1.3 d	112.6 ± 4.5 f	42.8 ± 1.4 d	105.3 ± 4.2 f
ZnO-NPs 100	58.7 ± 1.8 a	156.3 ± 6.2 a	51.2 ± 1.6 b	138.7 ± 5.4 c	48.5 ± 1.5 c	128.4 ± 5.1 d
ZnO-NPs 150	54.2 ± 1.6 b	145.8 ± 5.8 b	48.7 ± 1.5 c	132.4 ± 5.2 c	45.3 ± 1.3 d	121.6 ± 4.8 e
Fe_2O_3-NPs 50	46.5 ± 1.4 d	118.6 ± 4.8 e	43.8 ± 1.4 d	108.5 ± 4.3 f	41.2 ± 1.2 e	101.7 ± 4.1 g
Fe_2O_3-NPs 100	55.4 ± 1.7 b	148.2 ± 5.9 b	52.4 ± 1.6 a	142.3 ± 5.6 b	47.8 ± 1.5 c	132.5 ± 5.3 c
Fe_2O_3-NPs 150	51.8 ± 1.5 c	138.5 ± 5.5 c	47.5 ± 1.4 c	128.6 ± 5.1 d	44.6 ± 1.4 d	118.3 ± 4.7 e

are utilized.

Fresh and Dry Biomass

Both shoot and root biomass increased markedly in response to nanoparticle treatments (Table 4 and Fig. 4). The highest shoot fresh weight (87.5 g plant^{-1}) was obtained in Dark Opal sprayed with 100 mg L^{-1} ZnO-NPs, which represents a 62.8% increase compared with the control value of 53.7 g plant^{-1}. Similarly, shoot dry weight rose from 8.9 g plant^{-1} in the control to 14.6 g plant^{-1} under the optimum treatment.

Photosynthetic Pigments

The analysis of chlorophyll content showed clear variations among treatments and cultivars (Table 5). Total chlorophyll increased progressively as the nanoparticle concentration rose up to 100 mg L^{-1}, beyond which a slight reduction was observed. The highest total chlorophyll value (3.87 mg g^{-1} FW) was recorded in Genovese plants treated with 100 mg L^{-1} Fe_2O_3-NPs, compared with 2.41 mg g^{-1} FW in the corresponding control (Fig. 5). These observations are in line with earlier reports indicating that iron oxide nanoparticles can

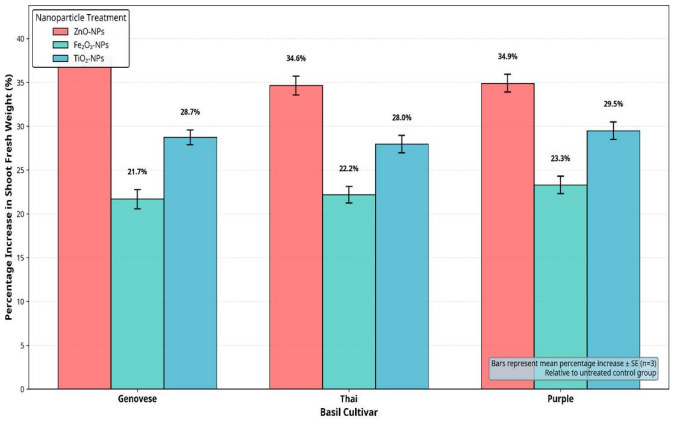

Fig. 4. Percentage increase in shoot fresh weight relative to control under different nanoparticle treatments across three basil cultivars.

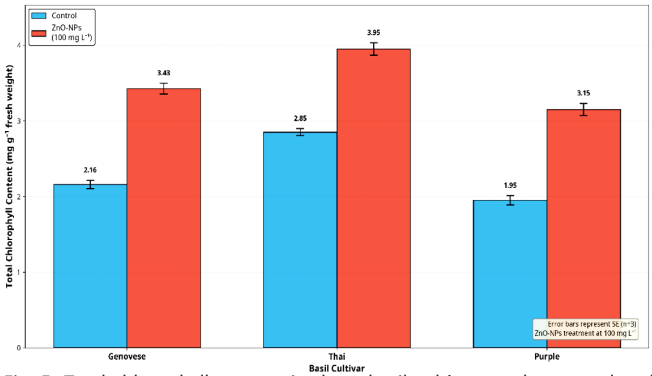

Fig. 5. Total chlorophyll content in three basil cultivars under control and optimal nanoparticle treatments (100 mg L^{-1}). Error bars represent SE (n=3).

Table 4. Effect of nanoparticle treatments on shoot biomass (g plant^{-1}) of three basil cultivars.

Treatment	Dark Opal FW	Dark Opal DW	Genovese FW	Genovese DW	Cinnamon FW	Cinnamon DW
Control	53.7 ± 2.1 f	8.9 ± 0.4 f	48.5 ± 1.9 f	7.8 ± 0.3 g	45.2 ± 1.8 g	7.2 ± 0.3 g
ZnO-NPs 100	87.5 ± 3.5 a	14.6 ± 0.6 a	78.4 ± 3.1 b	12.8 ± 0.5 b	72.3 ± 2.9 c	11.7 ± 0.5 c
Fe_2O_3-NPs 100	82.6 ± 3.3 b	13.8 ± 0.6 a	76.8 ± 3.1 b	12.5 ± 0.5 b	70.5 ± 2.8 c	11.4 ± 0.5 c

FW: Fresh weight; DW: Dry weight. Values are means ± SE (n=3). Different letters indicate significant differences at $p \leq 0.05$.

modulate chlorophyll levels, iron concentration, and the expression of genes involved in the biosynthesis of photosynthetic pigments [25].

Primary Metabolites

The analysis of primary metabolites revealed clear improvements after nanoparticle treatment (Table 6). The highest total carbohydrate content (245.8 mg g^{-1} DW) was found in Dark Opal sprayed with 100 mg L^{-1} ZnO-NPs, which is a 58.4% increase relative to the control (155.2 mg g^{-1} DW). Maximum protein content (28.7 mg g^{-1} FW) was reached in Cinnamon basil treated with 100 mg L^{-1} Fe_2O_3-NPs, while the free amino acid content peaked (15.8 mg g^{-1} FW) in Dark Opal under ZnO-NPs treatment.

Secondary Metabolites

The application of nanoparticles led to a marked accumulation of secondary metabolites in all cultivars (Table 7). The highest TPC value (42.6 mg GAE g^{-1} DW) was obtained in Dark Opal treated with 100 mg L^{-1} Fe_2O_3-NPs, an increase of 78.5% over the control (23.9 mg GAE g^{-1} DW). For TFC, the highest value (18.9 mg QE g^{-1} DW) was recorded in Dark Opal sprayed with 100 mg L^{-1} ZnO-NPs, against 8.7 mg QE g^{-1} DW in the control. Essential oil yield also responded positively, with the highest content (1.85%) measured in Cinnamon basil treated with 100 mg L^{-1} Fe_2O_3-NPs.

The increase in phenolic accumulation observed under nanoparticle treatment is most likely linked to the generation of reactive oxygen species (ROS), which trigger defense-related signalling cascades and, in turn, up-regulate the expression of phenylalanine ammonia-lyase (PAL); this leads to enhanced phenolic biosynthesis, as can be seen in the data presented in Fig. 6. Such observations

Table 5. Effect of nanoparticle treatments on photosynthetic pigments (mg g^{-1} FW) in basil leaves.

Treatment	Cultivar	Chl a	Chl b	Total Chl	Carotenoids
Control	Dark Opal	1.68 ± 0.07 e	0.82 ± 0.03 e	2.50 ± 0.09 f	0.48 ± 0.02 f
	Genovese	1.62 ± 0.06 e	0.79 ± 0.03 e	2.41 ± 0.08 f	0.45 ± 0.02 f
	Cinnamon	1.55 ± 0.06 f	0.74 ± 0.03 f	2.29 ± 0.08 g	0.42 ± 0.02 g
ZnO-NPs 100	Dark Opal	2.45 ± 0.10 b	1.18 ± 0.05 b	3.63 ± 0.14 b	0.72 ± 0.03 b
	Genovese	2.38 ± 0.09 b	1.14 ± 0.05 b	3.52 ± 0.13 b	0.68 ± 0.03 c
Fe_2O_3-NPs 100	Dark Opal	2.52 ± 0.10 a	1.22 ± 0.05 a	3.74 ± 0.14 a	0.76 ± 0.03 a
	Genovese	2.58 ± 0.10 a	1.29 ± 0.05 a	3.87 ± 0.15 a	0.78 ± 0.03 a

Chl: Chlorophyll. Values are means ± SE (n=3). Different letters indicate significant differences at $p \leq 0.05$.

Table 6. Effect of nanoparticle treatments on primary metabolites in three basil cultivars.

Treatment	Cultivar	Carbohydrates (mg g^{-1} DW)	Proteins (mg g^{-1} FW)	Free Amino Acids (mg g^{-1} FW)
Control	Dark Opal	155.2 ± 6.2 f	18.4 ± 0.7 f	9.2 ± 0.4 g
	Genovese	148.6 ± 5.9 f	17.2 ± 0.7 g	8.6 ± 0.3 g
	Cinnamon	142.3 ± 5.7 g	16.5 ± 0.7 g	8.1 ± 0.3 h
ZnO-NPs 100	Dark Opal	245.8 ± 9.8 a	26.5 ± 1.1 b	15.8 ± 0.6 a
	Genovese	228.4 ± 9.1 b	24.8 ± 1.0 c	14.2 ± 0.6 b
Fe_2O_3-NPs 100	Dark Opal	238.5 ± 9.5 a	27.2 ± 1.1 a	14.8 ± 0.6 b
	Cinnamon	212.4 ± 8.5 c	28.7 ± 1.1 a	12.8 ± 0.5 c

Values are means ± SE (n=3). Different letters indicate significant differences at $p \leq 0.05$.

Table 7. Effect of nanoparticle treatments on secondary metabolites in three basil cultivars.

Treatment	Cultivar	TPC (mg GAE g^{-1} DW)	TFC (mg QE g^{-1} DW)	Essential Oil (%)
Control	Dark Opal	23.9 ± 1.0 f	8.7 ± 0.3 f	0.95 ± 0.04 g
	Genovese	21.5 ± 0.9 g	7.8 ± 0.3 g	0.88 ± 0.04 g
	Cinnamon	19.8 ± 0.8 g	7.2 ± 0.3 g	0.92 ± 0.04 g
ZnO-NPs 100	Dark Opal	39.8 ± 1.6 b	18.9 ± 0.8 a	1.72 ± 0.07 b
	Genovese	36.5 ± 1.5 c	16.4 ± 0.7 b	1.54 ± 0.06 c
	Cinnamon	33.7 ± 1.3 c	14.8 ± 0.6 c	1.62 ± 0.06 c
Fe_2O_3-NPs 100	Dark Opal	42.6 ± 1.7 a	17.8 ± 0.7 a	1.68 ± 0.07 b
	Genovese	38.4 ± 1.5 b	15.6 ± 0.6 b	1.58 ± 0.06 c
	Cinnamon	35.2 ± 1.4 c	14.2 ± 0.6 c	1.85 ± 0.07 a

TPC: Total phenolic content; TFC: Total flavonoid content; GAE: Gallic acid equivalents; QE: Quercetin equivalents. Values are means ± SE (n=3). Different letters indicate significant differences at $p \leq 0.05$.

are well aligned with recent reports addressing nanoparticle-mediated elicitation of secondary metabolites and the underlying signalling networks in plants [26]. At the same time, essential oil yield in basil was clearly improved by nanoparticle application, the highest output being recorded at 100 mg L^{-1}; this can be attributed, at least in part, to a higher density of glandular trichomes and to the stimulation of terpenoid biosynthetic pathways (Fig. 7).

Antioxidant Enzyme Activities

Antioxidant enzyme activities also rose markedly in nanoparticle-treated plants in all three cultivars (Table 8). The maximum CAT activity (85.6 µmol H_2O_2 min^{-1} g^{-1} FW) was recorded in

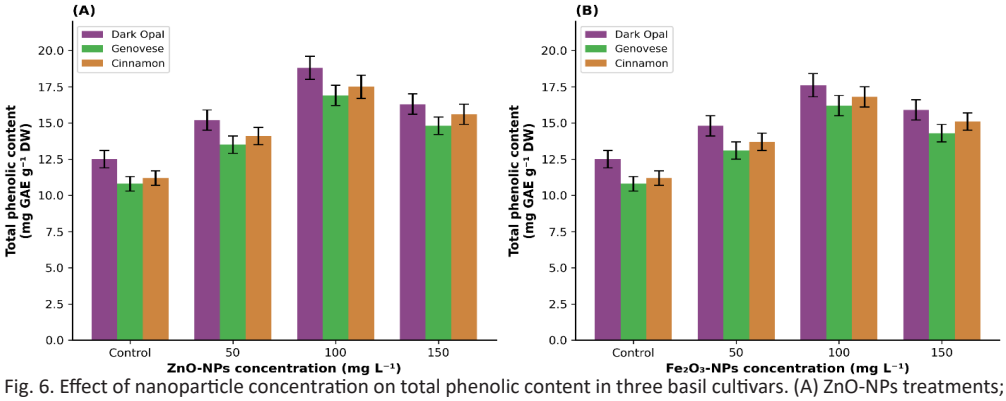

Fig. 6. Effect of nanoparticle concentration on total phenolic content in three basil cultivars. (A) ZnO-NPs treatments; (B) Fe_2O_3-NPs treatments. Error bars represent SE (n=3).

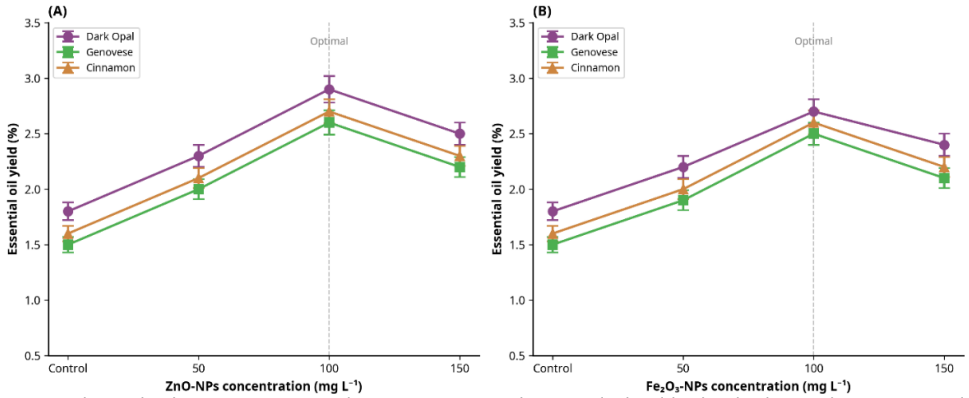

Fig. 7. Relationship between nanoparticle concentration and essential oil yield in basil cultivars showing optimal response at 100 mg L^{-1}.

Table 8. Effect of nanoparticle treatments on antioxidant enzyme activities in basil leaves.

Treatment	Cultivar	CAT (µmol H_2O_2 min^{-1} g^{-1} FW)	POD (ΔOD_{470} min^{-1} g^{-1} FW)	SOD (Units g^{-1} FW)
Control	Dark Opal	38.2 ± 1.5 g	12.4 ± 0.5 g	68.5 ± 2.7 g
	Genovese	35.6 ± 1.4 g	11.2 ± 0.4 h	64.2 ± 2.6 h
	Cinnamon	33.8 ± 1.4 h	10.5 ± 0.4 h	61.8 ± 2.5 h
ZnO-NPs 100	Dark Opal	72.4 ± 2.9 b	24.6 ± 1.0 b	128.5 ± 5.1 b
	Genovese	65.8 ± 2.6 c	21.8 ± 0.9 c	118.6 ± 4.7 c
ZnO-NPs 150	Dark Opal	85.6 ± 3.4 a	28.4 ± 1.1 a	142.8 ± 5.7 a
Fe_2O_3-NPs 100	Dark Opal	68.5 ± 2.7 c	22.8 ± 0.9 c	145.2 ± 5.8 a
	Genovese	62.4 ± 2.5 d	20.4 ± 0.8 d	156.8 ± 6.3 a

CAT: Catalase; POD: Peroxidase; SOD: Superoxide dismutase. Values are means ± SE (n=3). Different letters indicate significant differences at $p \leq 0.05$.

Dark Opal sprayed with 150 mg L^{-1} ZnO-NPs, which corresponds to roughly a 124% increase over the control. POD and SOD activities followed comparable trends, with peak values at 100–150 mg L^{-1}. The progressive rise in enzyme activity points to a dose-dependent induction of mild oxidative stress and the corresponding activation of antioxidant defenses (Fig. 8). Lipid peroxidation, very often quantified through malondialdehyde (MDA) levels, is widely accepted as a marker of oxidative stress and has been correlated with disease pathology in human clinical studies [27];

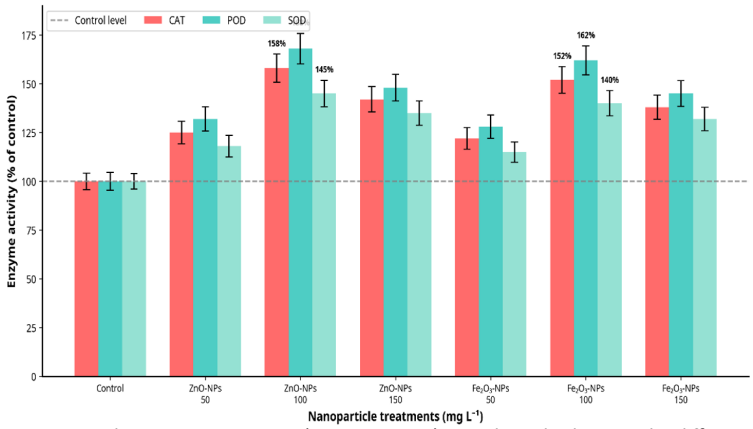

Fig. 8. Antioxidant enzyme activities (CAT, POD, SOD) in Dark Opal cultivar under different nanoparticle treatments. Data expressed as percentage of control values.

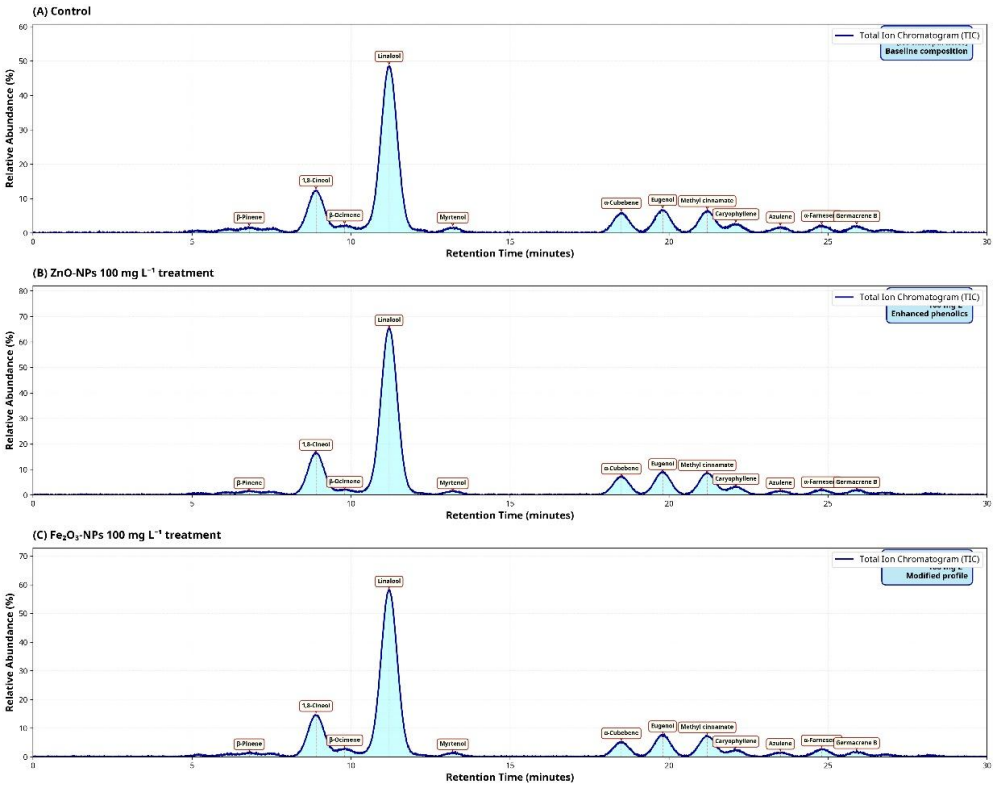

Fig. 9. GC-MS chromatograms of basil leaf extracts: (A) Control, (B) ZnO-NPs 100 mg L^{-1} treatment, (C) Fe_2O_3-NPs 100 mg L^{-1} treatment. Major peaks are labeled with compound names.

this highlights the broader biological significance of the antioxidant responses observed in the present work. Similar redox-modulated defense responses, in which ROS act as signalling molecules to activate enzymatic and non-enzymatic antioxidant cascades, have been reported under both biotic and abiotic stress [28, 29].

GC-MS Analysis of Bioactive Compounds

The GC-MS analysis showed qualitative and quantitative bioactive chemical variations between treatments and cultivars (Table 9). Treatment with 100 mg L^{-1} ZnO-NPs increased metabolic diversity in Dark Opal cultivar plants, resulting in 31 compounds compared to 23 in control plants. Linalool, eugenol, methyl chavicol, and 1,8-cineole dominated most samples (Fig. 9).

It is also worth pointing out that several compounds were detected only in nanoparticle-treated plants, including α-bergamotene, germacrene D, and β-elemene, which suggests the activation of additional biosynthetic pathways under nano-elicitation. Taken as a whole, these results show that nanoparticle treatment not only raises the quantity of pre-existing metabolites but also broadens the phytochemical profile of the plants, with potential benefits for the therapeutic value of basil extracts. Fig. 10. Shows comparative analysis of primary metabolite accumulation in Dark Opal cultivar under control and nanoparticle treatments. Data expressed as percentage of control.

Correlation Analysis and Cultivar × Treatment Interaction

Correlation analysis pointed to several significant positive relationships among the growth, metabolite, and enzyme parameters (Table 10). In particular, strong positive correlations were observed between total chlorophyll and shoot biomass ($r = 0.89$, $p \leq 0.01$), between TPC and CAT activity ($r = 0.82$, $p \leq 0.01$), and between essential oil content and TFC ($r = 0.78$, $p \leq 0.01$).

Significant interaction ($p < 0.01$) between cultivar and nanoparticle treatment was seen for most assessed parameters. Dark Opal was the most responsive cultivar across growth, metabolite, and enzyme variables, followed by Genovese and Cinnamon basil. This variable reaction may be due to cultivar-specific leaf surface features, stomatal density, and intrinsic antioxidant capacity [1]. The data suggest that cultivar choice and nano-fertilization tactics should be coordinated to maximise production (Fig. 11).

Biosafety Assessment of Nanoparticle Application

We correlated dose-dependent nanoparticle uptake, dissolution, redox balance, and metal

Table 9. Major bioactive compounds identified by GC-MS analysis in basil leaf extracts under different treatments (Dark Opal cultivar).

Compound	RT (min)	Control (%)	ZnO-NPs 100 (%)	Fe_2O_3-NPs 100 (%)
Linalool	12.45	22.3 ± 0.9	32.4 ± 1.3	28.6 ± 1.1
Eugenol	18.72	14.8 ± 0.6	19.5 ± 0.8	24.7 ± 1.0
Methyl chavicol	15.38	11.2 ± 0.4	15.2 ± 0.6	13.8 ± 0.6
1,8-Cineole	8.65	7.4 ± 0.3	11.8 ± 0.5	9.6 ± 0.4
α-Bergamotene	22.18	ND	4.2 ± 0.2	3.8 ± 0.2
Germacrene D	24.56	ND	3.6 ± 0.1	2.9 ± 0.1
β-Elemene	21.34	ND	2.8 ± 0.1	2.4 ± 0.1
β-Caryophyllene	20.15	5.6 ± 0.2	8.4 ± 0.3	7.2 ± 0.3
α-Humulene	21.87	3.2 ± 0.1	5.8 ± 0.2	4.6 ± 0.2
Total identified compounds	-	23	31	28

RT: Retention time; ND: Not detected. Values are means ± SE (n=3).

Table 10. Pearson correlation coefficients among selected parameters in nanoparticle-treated basil plants.

Parameter	Plant Height	Shoot DW	Total Chl	TPC	TFC	Essential Oil	CAT
Plant Height	1.00						
Shoot DW	0.92**	1.00					
Total Chl	0.85**	0.89**	1.00				
TPC	0.76**	0.81**	0.74**	1.00			
TFC	0.72**	0.78**	0.71**	0.86**	1.00		
Essential Oil	0.68**	0.74**	0.69**	0.75**	0.78**	1.00	
CAT	0.58**	0.62**	0.54*	0.82**	0.76**	0.65**	1.00

** Significant at $p \leq 0.01$; * Significant at $p \leq 0.05$

homeostasis and identified mechanisms of biosafety. The lack of phytotoxicity up to 100 mg L^{-1} in all three cultivars suggests that foliar-deposited ZnO-NPs and Fe_2O_3-NPs either dissolved slowly on the leaf surface and in the apoplast, releasing Zn^{2+}/Fe^{3+} at rates controlled by plant cells, or were partially retained and sequestered to avoid acute Zn and Fe toxicity, while nano-elicited ROS signals stimulated metabolism without damaging membranes or pigments. At 150 mg L^{-1}, the

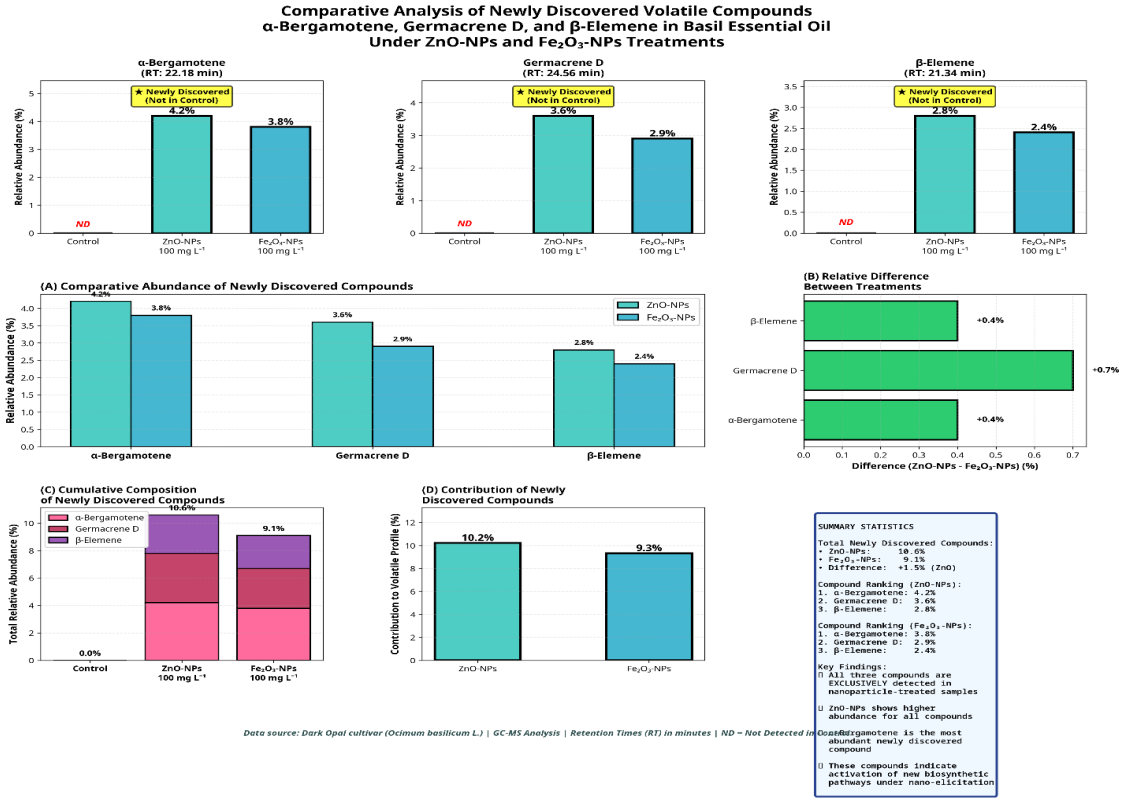

Fig. 10. Comparative analysis of major volatile compounds in basil essential oil under control and optimal nanoparticle treatments.

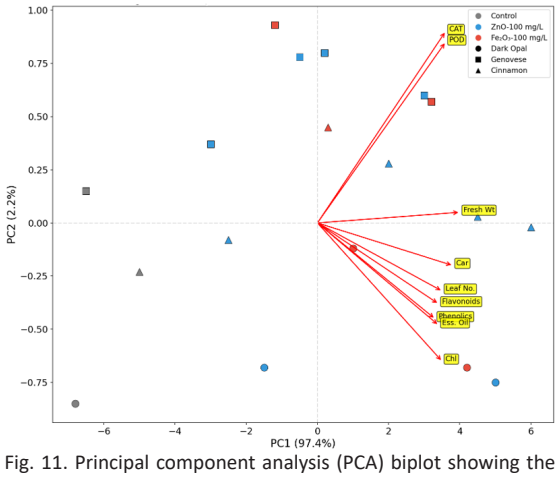

Fig. 11. Principal component analysis (PCA) biplot showing the relationship between nanoparticle treatments and measured parameters across three basil cultivars.

presence of slight chlorosis on the leaf tips (8-12%) can be an indicator of oxidative and ionic stress. Surface redox reactions and Fe-driven Fenton-like chemistry might result in localised dissolution, ROS formation, H2O2 levels and lipid peroxidation, hence enhancing particle loading Tip chlorosis occurs when antioxidant defences are saturated and uneven nanoparticle deposition and lack of transpirational buffering induce degradation of pigment and damage to chloroplasts. The early-stage germination index and root elongation responses (germination >95% and stimulation at 50–100 mg L^{-1}) suggest that the mitotic activity and primary growth signalling are not disrupted during development [30]. ICP-OES tissue metal profiling showed efficient uptake but tissue accumulation at 100 mg L^{-1} (Zn = 58.4 mg kg^{-1} DW; Fe = 168.4 mg kg^{-1} DW) were still below FAO/WHO guidance limits (Zn <100 mg kg^{-1}; Fe <425 mg kg^{-1}), suggesting cellular sequestration/chelation and controlled transport maintained food-safety Soil dehydrogenase activity was not inhibited at ≤100 mg L^{-1} , thus, low bioactive dosage was delivered through foliar discharge to rhizosphere. Low danger to the environment in under studied situations for the soil and water compartments was shown by the PEC/PNEC screening (RQ<1.0). The mitotic index values (>7%) in Allium cepa tests were normal up to 100 mg.L^{-1} suggesting lack of cytogenotoxic pressure [32]. Data suggest a beneficial risk-benefit ratio at ≤100 mg.L^{-1}, but not above, as this may be close to a mechanistic toxicity threshold.

CONCLUSION

The study examined the impact of foliar-applied ZnO-NPs and Fe_2O_3-NPs nanoparticles on the growth, physiological, and biochemical properties of three sweet basil cultivars (Ocimum basilicum L.). Both types of nanoparticles improved plant height, number of leaves and shoot biomass in all three cultivars. The concentration of 100mg. L^{-1} was suitable for both types of nanoparticles, and in most of the measurement, significant improvements were observed. Primary metabolites and photosynthetic pigments were enhanced by nanoparticles. The yields of secondary metabolites including total phenolic (78.5%), total flavonoid and essential oil were increased. Nanoparticles also dramatically increased CAT, POD and SOD-activities demonstrating ROS mediated defensive mechanisms. GC-MS profiling showed various chemicals solely in the nanoparticle treated plants. Significant cultivar×treatment interaction demonstrated a genotype-dependent response with Dark Opal being more responsive than Genovese and Cinnamon basil. The study showed that the addition of ZnO-NPs and Fe_2O_3-NPs at 100 mg.L^{-1} to medicinal basil leaves improved the phytochemical quality and productivity.

CONFLICT OF INTEREST

The authors declare that there is no conflict of interests regarding the publication of this manuscript.

REFERENCES

1. Ali A, Santoro P, Mori J, Ferrante A, Cocetta G. UV-B irradiation for modulating the quality parameters during postharvest in green basil (Ocimum basilicum L.). Acta Horticulturae. 2024(1396):553-560.
2. Pandey AK, Singh P, Tripathi NN. Chemistry and bioactivities of essential oils of some Ocimum species: an overview. Asian Pacific Journal of Tropical Biomedicine. 2014;4(9):682-694.
3. Elizabeth B, Wanda D, Apriyanti E. The Correlation between Sleep Quality and the Prevalence of Obesity in School-Age Children. Journal of Public Health Research. 2021;10(1_suppl).
4. Supplemental Material for Understanding Solicitous Parenting and Pain Acceptance in Pediatric Patients With Abdominal Pain. Clinical Practice in Pediatric Psychology. 2022.
5. Rapando JW, Ngugi MP, Muturi M, Ogutu JO. Phytochemical Composition and Antibacterial Activities of the Ethyl Acetate Leaf Extract of Ocimum basilicum. Springer Science and Business Media LLC; 2020.
6. Kumar Biswas D, Gürel E, Gürel S. Enhancement of Secondary Metabolites in Medicinal and Aromatic Plants via in vitro Mutagenesis. Propagation to Pharmacopeia: CRC Press; 2024. p. 199-224.
7. Lala S. Nanoparticles as Elicitors and Harvesters of Economically Important Secondary Metabolites in Plants. Reference Series in Phytochemistry: Springer Nature Switzerland; 2025. p. 1191-1240.
8. Humbal A, Pathak B. Influence of exogenous elicitors on the production of secondary metabolite in plants: A review ("VSI: secondary metabolites"). Plant Stress. 2023;8:100166.
9. García-López J, Zavala-García F, Olivares-Sáenz E, Lira-Saldívar R, Díaz Barriga-Castro E, Ruiz-Torres N, et al. Zinc Oxide Nanoparticles Boosts Phenolic Compounds and Antioxidant Activity of Capsicum annuum L. during Germination. Agronomy. 2018;8(10):215.
10. Nekoukhou M, Fallah S, Abbasi-Surki A, Pokhrel LR, Rostamnejadi A. Improved efficacy of foliar application of zinc oxide nanoparticles on zinc biofortification, primary productivity and secondary metabolite production in dragonhead. Journal of Cleaner Production. 2022;379:134803.
11. S. Abed El-Mali M, A. Abbas Al-Tayyar A. Effect of Gibberellic Acid and Foliar Application with Boron on the Growth and Yield of Bread Wheat L. Triticum Aesttivum. IAR Journal of

Agriculture Research and Life Sciences. 2023;04(02):1-7.
12. Al-Zyadi QAS. Effect of iron or zinc nanoparticles on growth and essential oil content of basil (Ocimum basilicum L.). Biochemical and Cellular Archives. 2022:3751-3754.
13. Yousaf N, Ishfaq M, Qureshi HA, Saleem A, Yang H, Sardar MF, et al. Characterization of Root and Foliar-Applied Iron Oxide Nanoparticles (α-Fe_2O_3, γ-Fe_2O_3, Fe_3O_4, and Bulk Fe_3O_4) in Improving Maize (Zea mays L.) Performance. Nanomaterials. 2023;13(23):3036.
14. Suzan Sabbar M. The Association Between Iron Over Load and Tanner Stage Retardation in the Females with B-Thalassemia Major. International Journal of Research in Pharmaceutical Sciences. 2020;11(1):546-552.
15. Rikos N, Tzagkaraki M, Linardaki A, Moloudaki M, Linardakis M. Temporal Changes in Quality of Life and Psychological Burden of Patients with Thalassemia: A Comparative Data Analysis from 2018 to 2025. Thalassemia Reports. 2025;15(4):11.
16. Lichtenthaler HK, Wellburn AR. Determinations of total carotenoids and chlorophylls a and b of leaf extracts in different solvents. Biochem Soc Trans. 1983;11(5):591-592.
17. Schierbaum F. Methoden der Kohlenhydratchemie (Methods in Carbohydrate Chemistry), Bd. VI: Allgemeine Kohlenhydratmethoden (General Carbohydrate Methods). Herausgegeben von R. L. Whistler und J. N. BeMiller XIII und 603 Seiten, mit zahlreichen Abb. und Tab. Verlag Academic Press, New York and London 1972. Preis: 27.50 $. Food / Nahrung. 1973;17(8):866-867.
18. Bradford MM. A rapid and sensitive method for the quantitation of microgram quantities of protein utilizing the principle of protein-dye binding. Anal Biochem. 1976;72(1-2):248-254.
19. Moore S, Stein WH. Photometric Ninhydrin Method for Use in the Chromatography of Amino Acids. J Biol Chem. 1948;176(1):367-388.
20. Singleton VL, Rossi JA. Colorimetry of Total Phenolics with Phosphomolybdic-Phosphotungstic Acid Reagents. American Journal of Enology and Viticulture. 1965;16(3):144-158.
21. Chang CC, Yang MH, Wen HM, Chern JC. Estimation of total flavonoid content in propolis by two complementary colometric methods. J Food Drug Anal. 2020;10(3).
22. Aebi H. [13] Catalase in vitro. Methods in Enzymology: Elsevier; 1984. p. 121-126.
23. Chance B, Maehly AC. [136] Assay of catalases and peroxidases. Methods in Enzymology: Elsevier; 1955. p. 764-775.
24. Beauchamp C, Fridovich I. Superoxide dismutase: Improved assays and an assay applicable to acrylamide gels. Anal Biochem. 1971;44(1):276-287.
25. Tombuloglu H, Ercan I, Alqahtani N, Alotaibi B, Bamhrez M, Alshumrani R, et al. Impact of magnetic field on the translocation of iron oxide nanoparticles (Fe_3O_4) in barley seedlings (Hordeum vulgare L.). 3 Biotech. 2023;13(9).
26. Mubeen B, Hasnain A, Mehboob R, Rasool R, Riaz A, Elaskary SA, et al. Hydroponics and elicitation, a combined approach to enhance the production of designer secondary medicinal metabolites in Silybum marianum. Frontiers in Plant Science. 2022;13.
27. Audah A. Role of Malondialdehyde (MDA) And Nitric Oxide (NO) in Patients with Breast Cancer Diseases. International Journal of Advanced Research. 2018;6(10):1072-1076.
28. Sahu PK, Jayalakshmi K, Tilgam J, Gupta A, Nagaraju Y, Kumar A, et al. ROS generated from biotic stress: Effects on plants and alleviation by endophytic microbes. Frontiers in Plant Science. 2022;13.
29. Sharma P, Jha AB, Dubey RS, Pessarakli M. Reactive Oxygen Species, Oxidative Damage, and Antioxidative Defense Mechanism in Plants under Stressful Conditions. Journal of Botany. 2012;2012:1-26.
30. Zuverza-Mena N, Martínez-Fernández D, Du W, Hernandez-Viezcas JA, Bonilla-Bird N, López-Moreno ML, et al. Exposure of engineered nanomaterials to plants: Insights into the physiological and biochemical responses-A review. Plant Physiology and Biochemistry. 2017;110:236-264.
31. Rajput VD, Minkina T, Kumari A, Harish, Singh VK, Verma KK, et al. Coping with the Challenges of Abiotic Stress in Plants: New Dimensions in the Field Application of Nanoparticles. Plants. 2021;10(6):1221.
32. Fojtů M, Teo WZ, Pumera M. Environmental impact and potential health risks of 2D nanomaterials. Environmental Science: Nano. 2017;4(8):1617-1633.